HHS Public Access

Author manuscript

Nat Struct Mol Biol. Author manuscript; available in PMC 2014 April 01.

Published in final edited form as:

Nat Struct Mol Biol. 2013 October ; 20(10): 1227–1235. doi:10.1038/nsmb.2665.

MicroRNA-based discovery of barriers to dedifferentiation of fibroblasts to pluripotent stem cells

Robert L Judson[1,2], **Tobias S Greve**[1,2], **Ronald J Parchem**[1,2], and **Robert Blelloch**[1,2]

[1]The Eli and Edythe Broad Center of Regeneration Medicine and Stem Cell Research, Center for Reproductive Sciences, Program in Biomedical Sciences, University of California San Francisco, San Francisco, California

[2]Department of Urology, University of California San Francisco, San Francisco, California

Abstract

Individual microRNAs (miRNAs) can target hundreds of messenger RNAs forming networks of presumably cooperating genes. To test this presumption, we functionally screened miRNAs and their targets in the context of de-differentiation of mouse fibroblasts to induced pluripotent stem cells (iPSCs). Along with the miR-302/miR-294 family, the miR-181 family arose as a novel enhancer of the initiation phase of reprogramming. Endogenous miR-181 miRNAs were transiently elevated with introduction of *Oct4*, *Sox2*, and *Klf4* (OSK), and their inhibition diminished iPSC colony formation. We tested the functional contribution of 114 individual targets of the two families, revealing twenty-five genes that normally suppress initiation. Co-inhibition of targets cooperatively promoted both the frequency and kinetics of OSK reprogramming. These data establish two of the largest functionally defined networks of miRNA-mRNA interactions, elucidating novel relationships among genes that act together to suppress early stages of reprogramming.

INTRODUCTION

MicroRNAs (miRNAs) are endogenous non-coding RNAs that regulate the translation of target genes. Together with Argonaute proteins, miRNAs form the RNA induced silencing complex (RISC) which suppresses messenger RNAs (mRNAs) by both inhibiting translation and accelerating degradation[1]. Targeting is largely determined by complementation of a 6-8 nucleotide seed sequence with the 3′ untranslated region (UTR) of the mRNA[2]. Single miRNAs can down-regulate hundreds of transcripts simultaneously[3–7]. Interestingly, the functional significance of this extensive parallel co-inhibition of gene networks, while the subject of much speculation, remains largely unexplored experimentally. Functional studies

Corresponding author: R Blelloch BlellochR@stemcell.ucsf.edu.

ACCESSION CODES: Pending

Author Contributions

R.L.J. contributed to Figs 1, 2, 3, 4a–e, 5, 6, 7a,f–g and Supplementary Figs 2-6. T.G. contributed to Figs 4d,f, 7b–e and Supplementary Figs 1, 2, 4 and 7. R.J.P. contributed to Figs 2b and Supplementary Figs 1 and 2. R.B. and R.L.J. conceived the experiments, analyzed the data, and wrote the manuscript.

generally focus on the regulation a small number of target genes known to be involved in the biological process of interest[8]. Frequently, knockdown of these individual targets recapitulates the phenotype of over-expressing the miRNA itself, leading to the "dominant target" hypothesis. However, as a miRNA's many mRNA targets were presumably evolutionarily selected to be co-regulated, a systematic dissection of these targets is likely to uncover a network of genes that function together rather than alone.

The evolutionary history of miRNAs suggests they play major roles in promoting specific cell fates in complex organisms[9,10]. We set out to functionally characterize the miRNA-mRNA interactions that promote the pluripotent cell fate using the assay of directed de-differentiation, also called reprogramming. During reprogramming, somatic cells are de-differentiated into induced pluripotent stem cells (iPSCs) via over-expression of defined transcription factors[11]. Reprogramming consists of two phases: initiation and maturation[12,13]. We chose to map functional miRNA-mRNA interactions in this system for three reasons. First, although several studies have dissected various aspects of the maturation phase, little is known about the early initiation phase where most reprogramming events are aborted[12–14]. Second, at least one family of miRNAs the embryonic stem cell enriched cell-cycle regulating (ESCC)-miRNAs, including miR-302 and miR-294 - potently regulates this transition[15–23]. Indeed, ESCC-miRNAs alone, or in combination with other miRNAs, have been shown to drive reprogramming in the absence of other reprogramming factors[18,19,23]. Thus, miRNA-mRNA interactions during reprogramming should offer insight into the mechanisms of this transition. Finally, we hypothesized that through mapping functional miRNA-mRNA interactions, we would identify networks of cooperating genes that could be manipulated with combinations of small molecules to enhance this transition.

RESULTS

ESCC and miR-181 miRNA families enhance OSK-reprogramming

We screened 570 chemically synthesized mature mouse miRNAs (mimics) for their ability to promote *Oct4* (*Pou5f1*), *Sox2* & *Klf4* (OSK)-induced reprogramming of mouse embryonic fibroblasts (MEFs). Although many combinations of reprogramming factors now exist, OSK-reprogramming offered two distinct advantages. First, OSK is the most frequently reported core set of required reprogramming factors, with *cMyc* being both dispensable and possessing transformative properties[24,25]. Second, OSK reprograms with consistent but low efficiency, resulting in a sensitive assay for identification of barriers to this transition. Indeed, miR-302's reprogramming enhancing properties were first discovered using this strategy[15]. We transfected individual wells of OSK-infected MEFs possessing an *Oct4-GFP* transgene with mimic on days 1 and 7 post-infection[26] (Fig. 1a). The mimics functioned for 6 days post-transfection as determined by a GFP-based miRNA-activity reporter (Supplementary Fig. 1). Therefore, serially transfected mimics should function throughout reprogramming. We compared the number of day 16 Oct4-GFP+ colonies in each mimic-containing well to 16 mock-transfected wells using strictly standardized mean difference (SSMD), a statistical parameter measuring both magnitude and confidence of effect size[27]. Sixteen mimics enhanced the frequency of Oct4-GFP+ colony formation in biological

duplicate screens (Fig. 1b and Supplementary Table 1a). OSK-mimic induced colonies were morphologically similar to mouse embryonic stem cells (mESCs) and expressed comparable levels of endogenous *Oct4*, *Sox2*, *Klf4*, *Rex1*, SSEA1 and NANOG (Supplementary Fig. 2a–b). Oct4-GFP+ colonies also silenced the exogenous retroviruses, indicating an advanced stage of reprogramming (Supplementary Fig. 2c).

Several of the miRNAs mimics that enhanced reprogramming shared a common seed sequence (Supplementary Table 1b). The most represented was the ESCC-miRNA seed sequence, validating the sensitivity of the screen (Fig. 1c). Indeed, even miR-467d, which contains a slightly diverged ESCC-miRNA seed sequence, enhanced OSK-reprogramming, consistent with previous reports that shifted or degenerate ESCC-miRNA seed sequences enhance reprogramming[22,28]. The second most enriched seed sequence was from the miR-181 family, not previously associated with reprogramming. Validation experiments confirmed the ability of the miR-181 family to enhance iPSC colony formation (Fig. 1c). OSK with miR-181 generated fully reprogrammed iPSCs with normal karyotypes, which contributed to all germ layers when injected into E3.5 blastocysts, including the germ line (Supplementary Fig. 2d–f). This screen confirmed the role of the ESCC-family of miRNAs as potent enhancers of reprogramming, and unveiled a similar ability for the miR-181 family.

miR-181 is a downstream mediator of OSK-reprogramming

The ESCC-miRNAs are expressed in pluripotent stem cells[29,30]. Similar to other pluripotency factors, such as *Oct4* or *Sox2*, their ectopic over-expression can drive reprogramming, although endogenous activation occurs late in the transition[14,15,23,31]. In contrast, neither MEFs nor pluripotent stem cells express high levels of miR-181[30]. Further, unlike the ESCC-miRNAs, which block mESC differentiation, expression of miR-181 destabilizes mESCs[32,33]. Interestingly, the promoter of the miR-181c&d locus is bound by OCT4, SOX2 and NANOG[31]. Previously reported miRNA profiling suggested dynamic regulation of the miR-181 family during OSK+*cMyc*-reprogramming. In one dataset, miR-181c and miR-181d are activated, but miR-181a and miR-181b suppressed, as MEFs transitioned to iPSCs[31]. In a second report, miR-181a was activated then subsequently silenced in iPSCs[14]. We measured miR-181 family expression during the course of OSK-reprogramming. Reverse transcription quantitative polymerase chain reaction (RT-qPCR) demonstrated an early induction of these miRNAs by OSK, which persisted throughout reprogramming, followed by silencing in iPSCs[34] (Fig. 2a). To determine the robustness and timing of endogenous miRNA activity, we generated GFP-based miRNA activity reporters for the miR-181 and ESCC-miRNA families as well as the let-7 family, which suppress reprogramming[32] (Supplementary Fig. 1). Notably, let-7 miRNAs are highly expressed in MEFs and not silenced until late in reprogramming while ESCC-miRNAs are absent in MEFs and not activated until late in reprogramming[14,15,30–32]. Consistent with the timing of their expression, the ESCC-miR reporter was active (miRNAs low), and the let-7 reporter silenced (miRNAs high), during early reprogramming (Fig. 2b). In contrast, the miR-181-activity reporter was silenced shortly after OSK introduction, reaching maximum suppression as early as 4 days, consistent with OSK-induced miR-181 expression (Fig. 2b). Inhibition of miR-181 with transfected inhibitors on days 1 and 5 post-OSK infection

reduced the number of day 16 Oct4-GFP+ colonies by 50-60%, showing that OSK functions, at least partially, through activation of endogenous miR-181 (Fig. 2c).

ESCC and miR-181 miRNAs promote the initiation phase

Previous studies have established at least two distinct phases of OSK+*cMyc* reprogramming[12,13]. Completion of the initiation phase is marked by a successful mesenchymal-to-epithelial transition (MET), but is otherwise poorly understood. Cells then enter the maturation phase, which has been characterized as a serial activation of the pluripotency hierarchy of transcription factors[13]. In OSK-reprogramming, a subpopulation of MEFs entered the maturation phase around day 8, as marked by the down-regulation of *Slug* and the activation of *Cdh1* and *Dnmt3l*[12] (Fig. 3a–c). The early activation and subsequent silencing of miR-181 suggests it functions during initiation. Similarly, the observation that ectopic introduction of ESCC-miRNAs alone can induce reprogramming, indicates that these miRNAs can independently initiate reprogramming[23]. To further evaluate when within reprogramming these miRNAs have their greatest effect, we conducted a time-course of single transfections. Populations of reprogramming cells are highly heterogeneous, and most cells do not complete initiation[13,14]. Therefore, transient miRNA mimics transfected on day 1 affect MEFs in initiation, whereas those transfected on day 9 affect a mixed population of cells both in initiation and in maturation (Fig. 3d). Introduction of miR-294 (an ESCC miRNA) and miR-181 at day 1 showed greater ability to enhance colony formation, as compared to introduction at later time points (Fig. 3e), suggesting that both miRNA families largely promote reprogramming during the initiation phase. Two further lines of evidence are consistent with this conclusion. First, we separated day 8 OSK-infected MEFs into initiation (CDH1-) and post-initiation (CDH1+) populations using flow cytometry, and transfected each population with mimic. miR-294, and miR-181 enhanced the number of day 20 Oct4-GFP+ colonies in the CDH1-, but not the CDH1+ populations (Fig. 3f). Second, we profiled gene expression on day 3 post-OSK-infection, 48 hours after the addition of miR-294 or miR-181[35,36]. Of the 3411 genes expressed significantly higher in iPSCs compared to MEFs, only 230 (6.7%) were up-regulated 3 days after addition of OSK and control mimic (Fig. 3g). Addition of miR-294 and miR-181 increased the number of up-regulated iPSC-specific genes to 15.2% and 8.5%, respectively. Similarly, we found 3754 genes with lower levels of expression in iPSCs as compared to MEFs, of which 372 (9.9%) were down-regulated by OSK and control mimic. Addition of miR-294 and miR-181 increased the set of iPSC-specific down-regulated genes to 15.4% and 10.7%, respectively. Together these data show that ectopic miR-294 and miR-181 promote iPSC production by regulating early reprogramming, and shift the transcriptional profile closer to that of fully-reprogrammed iPSCs as early as day 3, well before activation of the earliest maturation markers. Interestingly, the effects of miR-294 and miR-181 were not synergistic, suggesting that these miRNA families with different seed sequences, functionally converged down-stream (Fig 3h).

Functional miRNA-mRNA interactions during reprogramming

We next sought to dissect the mechanisms of reprogramming-enhancing miRNAs by knocking down individual targets. Previous attempts at defining the mechanism of the ESCC-miRNAs focused on a small number of targets selected based on expected roles in

reprogramming[16,17,21,23]. To take an unbiased approach, we generated a database of predicted targets for miR-294 and miR-181, based upon relationships of inverse expression, but not considering knowledge of function. We consolidated genes that were previously verified to be significantly down-regulated on the protein or mRNA level by over-expression of the miRNAs in various cell types[3,32,37–41]. We then retained genes that contained a predicted miRNA binding site. For down-regulated genes originally identified in human cells, we required this binding site to be conserved between human and mouse and have a high ranking context score (Targetscan, context score <−0.25)[42]. Finally, we required the genes to be expressed in MEFs, reprogramming MEFs, iPSCs or ESCs[32,43]. This process resulted in sets of 1079 and 58 genes for miR-294 and miR-181, respectively. Small interfering RNA (siRNA) pools (Dharmacon) were designed against all of the miR-181 targets, the 5% most down-regulated miR-294 targets (56 genes), and 54 random genes, with no over-lapping genes (Supplementary Table 2). We transfected MEFs one day after OSK-infection. At day 16 post-infection, 10 of the 56 miR-294 targets and 12 of the 58 miR-181 targets demonstrated significant increases in Oct4-GFP+ colony formation relative to four independent non-targeting siRNA control pools (p-value <0.01 and SSMD >2 over three independent experiments) (Fig. 4a and Supplementary Fig. 3). In contrast, only 3 of the random pools of siRNAs demonstrated similar effects. We verified siRNA knockdown by RT-qPCR (Fig. 4b). To rule out off-target effects of siRNAs, we tested independent pools targeting distinct gene regions. The independent pools showed highly effective knockdown of corresponding genes (Fig. 4b). Of the ten miR-294 targets identified in the original screen, eight (*Cdkn1a, Zfp148, Hivep2, Ddhd1, Dpysl2, Pten, Cfl2 and 9530068E07Rik*) confirmed using the independent siRNA pools (Fig. 4c). Similarly, eight of the original twelve miR-181 targets (*Bptf, Lin7c, Cpsf6, Nr2c2, Bclaf1, Nol8, Igfbp2, and Marcks*) verified. In contrast, knockdown of only one of the randomly selected genes consistently enhanced reprogramming, revealing a strong enrichment for genes that influence reprogramming among predicted targets of miR-294 and miR-181.

Cdkn1a is an established miR-294 target[44]. To determine whether the other identified genes were direct targets, we cloned gene-specific 3′UTRs containing miRNA binding sites into luciferase reporter constructs (Supplementary Fig. 4). We also generated constructs containing mutated binding sites, and assayed both reporters for mimic-induced luciferase repression (Fig. 4d). With the exception of Lin7c, the expected miRNAs inhibited translation of every wildtype, but not mutant, construct, indicative of direct miRNA targeting. We confirmed the suppression of the targets by the miRNAs in the context of OSK-reprogramming by RT-qPCR and Western blots. For most targets, RT-qPCR showed decreased mRNA levels on day 3 of reprogramming, 48 hours post transfection of the miRNA (Fig. 4e). Of the remaining five genes, antibodies to DPYSL2 and PTEN were available and showed diminished protein levels following miRNA introduction by Western blot (Fig. 4f). Further, inhibition of miR-181 during reprogramming caused a reciprocal upregulation of *Nr2c2* and *Marcks* by day 3 post-infection, demonstrating that these genes are targeted by OSK-activated endogenous miR-181 as well (Supplementary Fig. 5). Similar inhibition of the ESCC-miRNAs did not upregulate expression of targets, consistent with the lack of endogenous ESCC-miRNA activity during this time window (Supplementary Fig. 5).

Together, these experiments identified seventeen miRNA-regulated genes that are barriers to reprogramming.

During the course of these experiments, we noted a consistent difference between miR-294 and miR-181-enhanced OSK-reprogramming. Whereas the day 16 Oct4-GFP+ colonies in miR-181 conditions were generally the same size as with control mimic, the miR-294 conditions yielded significantly larger colonies (Fig. 5a). This divergence of phenotype was also observed with siRNAs against the miRNA targets; that is, miR-294-targeted genes increased both area and number of colonies while miR-181-targeted genes generally increased number (Fig. 5b). Further analysis of the screen data revealed siRNAs against six additional miR-294 targets and three additional miR-181 targets that increased only colony area, but not number (Fig. 5b & Fig. 4d). The increase in colony number is consistent with an increase in the number of successful initiation events. In contrast, we hypothesized that colony size could reflect either the kinetics of reprogramming or the proliferation rate of reprogramming cells. To test these two possibilities, we transfected both established iPSCs lines and OSK-reprogramming MEFs with miR-294 or miR-181, and measured colony growth rate. Neither mimic significantly altered partial or established iPSC colony growth rate (Fig. 5 c&d). In contrast, in both contexts, colony size was highly correlated with onset of colony appearance, supporting an interpretation of colony area as a surrogate measurement for the kinetics of reprogramming (Fig. 5e&f). These data demonstrate that the frequency and rate of reprogramming initiation events are separable processes that can be independently altered by these miRNAs and their targets.

We next asked whether multiple miRNA-mRNA functional interactions could cooperate to further influence colony number and/or area during reprogramming. We screened siRNAs against targets of individual miRNA for cooperative functionality by co-transfection of all pair-wise combinations on day 1 of OSK-reprogramming (Fig. 6a). For both families, between 16 and 40% of potential relationships were cooperative between two co-targeted siRNAs, but not between targeted siRNA and control siRNA (Fig. 6a&b). In contrast, we detected very few disruptive relationships. Together, these data show that miR-294 and miR-181 act to enhance reprogramming through a network of cooperating miRNA-mRNA interactions.

Functional miRNA-regulated pathways during reprogramming

As miR-294 and miR-181 did not show significant cooperation with each other (Fig. 3h), and shared no identified overlapping targets, we reasoned that two miRNA families might functionally converge on common signaling pathways or cellular processes. As our lists of functional target genes were too small to conduct pathway/cellular process enrichment analyses, we included high scoring computationally predicted targets (Targetscan, context score <−0.25)[42]. Among the top signaling pathways and processes predicted to be targeted by both miRNAs were Cadherin, Wnt, p53 and TGF-Beta signaling, as well as apoptosis and cell cycle regulation, each of which have been demonstrated to regulate reprogramming[45–48] (Supplementary Fig. 6a&b and Fig. 7a). We further identified additional pathways and processes, including several that influence Akt signaling. To evaluate whether the miRNAs regulate the predicted downstream pathways in this biological context, we tested the

influence of miR-294 or miR-181 on Akt, Wnt and TGF-Beta signaling during early reprogramming. MiR-294, but not miR-181, increased the ratio of IGF-activated phospho-AKT to total AKT on day 3 of reprogramming (Fig. 7b). Both miRNAs activated Wnt signaling during reprogramming as measured by TopFlash activity and nuclear localization of B-catenin[49] (Fig. 7c–d). Similarly, both miRNAs regulated TGF-Beta signaling as measured by decreased endogenous phosphorylated-SMAD2 during OSK reprogramming (Fig. 7e). These data demonstrate that during reprogramming initiation the ESCC and miR-181 families converge on TGF-Beta signaling inhibition and Wnt signaling activation, and the ESCC-miRNAs additionally activate Akt-signaling.

The above data suggests that alternative means of manipulating the miRNA targeted genes or pathways, specifically during reprogramming initiation, could increase the overall efficiency of iPSC production. *Prkaa1*, *Ddhd1*, *Cfl2*, *Pfn2*, and *Erap1* are interesting miR-294 targets as they demonstrate that directed manipulation of the metabolic circuit, cytoskeleton, and endoplasmic reticulum can actively enhance reprogramming. Therefore, we supplemented early OSK-reprogramming with small molecule inhibitors to *Prkaa1* (Compound C) and *Erap1* (Bestatin), and found that both also enhanced production of IPSC colonies (Supplementary Fig. 6c). We next focused on the identified signaling pathways. To manipulate Akt signaling, we expressed a tamoxifen-inducible active AKT (M+Akt:ER), or an inactive mutant (M−Akt:ER)[50]. Strikingly, the active AKT enhanced colony formation, specifically when tamoxifen was administered during reprogramming initiation (Supplementary Fig. 6d). These data corroborate our observation that siRNA against *Pten*, which inhibits Akt activity (Fig. 7b) also enhances reprogramming (Fig. 4c), consistent with two recent reports[51,52]. Likewise, recombinant WNT3A and a small molecule TGFBRI inhibitor (Tgfbr Inh), both known enhancers of reprogramming, functioned during the initiation phase (Supplementary Fig. 6e&f). Interestingly, whereas Akt and Wnt activation both exclusively functioned during the initiation phase, TGF-Beta inhibition functioned equally at both time-points. To test combinatorial effects of the pathways, we added activated M+Akt:ER, WNT3A, and Tgfbr Inh on days 2–8 of OSK-reprogramming. Increased Wnt and Akt signaling together did not further enhance colony formation suggesting redundant or converging roles of these pathways (Fig. 7f). Conversely, TGF-Beta signaling inhibition cooperated with both activated Wnt and Akt signaling (Fig. 7f). These data show that although miR-294 and miR-181 have independent targets that enhance reprogramming initiation, but converge on a subset of signaling pathways.

DISCUSSION

Together, this study identifies two miRNA families, 25 miRNA-mRNA interactions, three miRNA coordinated pathways and two small molecules that regulate the initiation phase of reprogramming, and can be used to manipulate distinct processes during this transition. Ectopic introduction of the ESCC family is a well-established enhancer of reprogramming, although the endogenous loci expressing ESCC-miRNAs are only activated late in the transition[15–23]. Here we uncover miR-181 as a novel enhancer to reprogramming and show that in contrast to the ESCC miRNAS, this family is activated shortly after the introduction of OSK and is not highly expressed in the final iPSC state. This transient expression is important for the reprogramming process, as knockdown of endogenous miR-181

suppressed iPSC formation. Endogenous miR-181 functions in part through the suppression of *Nr2c2* and *Marcks* as the transcript levels of these targets were elevated following miR-181 knockdown and siRNAs to these targets enhanced iPSC formation. Regardless of the timing of endogenous OSK-induced expression, the ectopic introduction of both families suppressed many targets and had the greatest effect when added early in reprogramming. Overall, we find that ectopically introduced miRNAs remove multiple barriers that inhibit the initiation phase of OSK-reprogramming. It should be noted that although extensive, our methods were not comprehensive, and other functional targets of ectopic or endogenous ESCC or miR-181 family miRNAs during reprogramming likely remain to be uncovered.

The multiple functional targets we uncover as barriers can be grouped into various cellular processes. Among these processes, cell cycle/senescence and apoptosis are previously identified barriers[20,53]. Here, we also identify cellular metabolism, membrane trafficking, and actin dynamics as additional barriers. Previous studies identified a shift in AMPK-regulated metabolic state between the starting fibroblast population and the final iPSC state, that, if blocked, inhibited the transition[54]. However, it was unclear whether inducing this shift would further aid in accelerating this transition. Our data, both using siRNAs and a small molecule inhibitor strongly support this conclusion. Determining how membrane trafficking influences the transition will be interesting endeavors for future studies. It has been shown that regulated membrane trafficking of collagen IV plays a critical role in maintaining the embryonic stem cell state without influencing the fibroblast state[55] We propose this example is just the tip of the iceberg in terms of the interconnection between membrane trafficking and the switch in cell state. Similarly, actin and cytoskeletal dynamics in regulating cell state is likely to be an important and expansive area of research. For example, our finding that *Cfl2* and *Pfn2* are barriers to de-differentiation suggests that inhibition of monomeric actin or the promotion of filamentous actin plays a critical role in the fibroblast to iPSC transition.

Our results show that many, if not most, of the barriers to de-differentiation are during the initiation phase of reprogramming. Our analysis following iPSC colonies over time enabled the measurement of two distinct types of barriers to reprogramming: one influencing the number of successful initiation events and the other the rate at which they occur. This separated the phenotypic consequences of target knockdown into three classes. One class predominantly reduces the total number of successful reprogramming events, while having little effect on the size of colonies, likely reflecting no overall change in the kinetics of the assay. Among the genes found in this set are *Cfl2*, *Bptf*, *Lin7c*, *Cpsf6*, *Nr2c2*, *Bclaf1*, *Nol8*, *Igf2bp2*, and *Marcks*. Another set of genes suppresses the kinetics of colony formation while having a much smaller effect on number. This set includes *Pfn2*, *Erap1*, *Ankrd52*, *Prkaa1*, *Lats2*, *Zbtb41*, *Foxk1*, *Metap1*, and *Atm*. Finally, there were a set of genes affecting both frequency and kinetics *including Cdkn1a*, *Zfp148*, *Hivep2*, *Ddhd1*, *Dpysl2*, *Pten*, and *9530068E07RIK*. The cellular basis for these different outcomes remains to be determined.

Importantly, our data show that at least in the context in reprogramming, there is no “dominant” target underlying an ectopically introduced miRNA’s ability to promote cell state transitions. Focusing on a large subset of targets of both the ESCC and miR-181 miRNA mimics, we find roughly twenty percent can in part explain each miRNAs’

mechanism. Most published studies have focused on individual targets, often suggesting a dominant target underlies the effect of the miRNA though it is established that an individual miRNA suppresses many targets simultaneously[3–6]. The “dominant target” model is based on the observation that knockdown or knockout of an individual target often completely recapitulates a miRNA over-expression phenotype. Indeed, we find many of the individual targets we tested largely recapitulate the capacity of the corresponding miRNAs to enhance reprogramming of fibroblasts to iPSCs. However, we were also able to see cooperative effects when targets were suppressed in pair-wise combinations. Therefore, that knockdown of many targets can have effects close to that of the miRNA likely reflects both a combination of redundant functions among targets as well as experimental artifact. In particular, experimentally induced knockdown is much greater than the suppression caused by the miRNA (typically less than a 50% diminishment of the target protein[3,4]. While our studies are largely focused on ectopic introduction of miRNAs during an induced transition, endogenous miRNAs are also known to have multiple targets[3]. Therefore, the combinatorial effect of multiple cooperating targets, rather than a few dominant targets, is unlikely to be unique to *in vitro* reprogramming, but instead relevant to most instances of miRNA regulation.

Ectopic introduction of miRNAs can have remarkable impacts on cell state transitions such as fibroblast dedifferentiation to iPSCs as well as the transdifferentiation of fibroblasts to neurons or cardiomyocytes[56–58]. However, genetic deletion of miRNAs largely have no dramatic effects in vivo under homeostatic conditions[59]. Therefore, it has been proposed that miRNAs are generally not required to establish or maintain cell states, but rather stabilize cell states against random noise and environmental perturbations, through inhibition of stochastic and aberrant gene expression[60]. Interestingly, reprogramming initiation has been characterized by its highly stochastic gene expression[13]. Consistent with the robustness model for miRNA function, our expression data show that the ectopically introduced miRNAs function to “focus” this early stochastic expression of genes toward patterns more similar to the iPSC profile, presumably by removing molecular barriers that would otherwise divert reprogramming cells away from the path to pluripotency (Fig. 7g). It will be important to determine if miRNAs will function similarly in other cell state transitions.

ON-LINE METHODS

Cell Culture

MEF Generation—MEF generation was conducted as previously described[26]. In brief, either rosa26-Bgal;Oct4-GFP or Oct4-GFP embryos were harvested on E13.5. Heads and visceral tissue were removed. Remaining tissue was disassociated with trypsin and physical disruption and plated (P0) in MEF media (high glucose (H-21) DMEM, 10%FBS, non-essential amino acids, L-glutamine, Penn/Strep, 55uM beta-mercaptoethanol). MEFs were expanded to P3 and frozen.

Virus Production—HEK293T cells grown to approximately 70% confluence were transfected with pCL-Eco and pMXs- or pWZL-expression plasmids at a ratio of 1:2 following the Fugene 6 manufacture’s protocol. At 24 hours, media was replaced with fresh

MEF media. At 48 hours, supernatant was harvested, filtered (0.45uM) and frozen at -80 degrees. Virus preparations were only thawed once before use.

Lentivirus: HEK293T cells grown to approximately 70% confluence were transfected with pMDL, pRSV, pVSVG and pSIN-expression plasmids at a ratio of 1:1:1:2 following the Fugene 6 manufacture's protocol. Cells were left for 48 hours, then harvested as above.

De-differentiation—Oct4-GFP MEFs (P5) were plated onto gelatin coated Whatman Clear View or Greiner uClear black-walled 96-well imaging plates at 900 cells / well. The next day, 50ul of each retrovirus-containing supernatant with 4ug/mL polybrene was added. Day 1 post infection, virus was replaced with fresh MEF media. Thereafter, media was changed every other day, with ES+FBS media (15%FBS, non-essential amino acids, L-glutamine, Penn/Strep, 55uM beta-mercaptoethanol and Lif) days 2 to 6 post-infection and ES+KSR media [Knock-out DMEM (Invitrogen), 15% Knock-out Serum Replacement (Invitrogen), non-essential amino acids, L-glutamine, Pen/Strep, 55uM beta-mercaptoethanol and Lif] days 6 to 16 post-infection. Supplements were added at indicated final concentrations: Tamoxifen (Sigma, 1nM), recombinant Wnt3a (R&D Biosystems, 50ng/mL), E-616452 (BioVision, TgfbR inhibitor, "RepSox", 1uM), Compound C (Sigma, AMPK inhibitor, 400pg/mL), Bestatin (Sigma, 250nM). Oct4-GFP expression and colony formation was assessed on days indicated, usually day 16 post-infection. High throughput imaging and high content analysis were conducted with the InCell Analyzer 2000 imaging station and software suit (GE). For screens, colony counts and measurements were automated. Independent experiments are defined as independent MEF lots infected with independent virus preparations. To validate pluripotency, day 16 iPSC colonies were disassociated with trypsin and plated onto irradiated MEF feeder layers (P1) and expanded. Passage 3 colonies were harvested for RT-qPCR and fixed for immunohistochemistry. Passage 5 colonies were injected into blastocysts.

Blastocyst Injection

Karyotyping and blastocyst injections to assay for chimeric contribution were performed as previously described[15,26]. Blastocysts were obtained from E2.5 super-ovulated and fertilized C57BL/6 females (Taconic). Blastocysts were washed in M2 media (Specialty Media) and grown in KSOM media (Specialty Media) for 16h. 16h after blastocyst collection, 10–15 iPS cells were injected into cultured blastocysts, which were then transplanted into the uteri of E2.5 pseudo-pregnant Swiss-Webster females (Taconic). For analysis of tissue contribution, embryos were collected on E13, and stained for B-gal activity. For analysis of germ line contribution, embryos were collected on E13 and gonads were isolated and imaged under fluorescence. 80% of implanted blastocysts demonstrated high-grade chimeric contribution of iPS lines.

Small RNA Transfections

MicroRNA mimics (MIRIDIAN), siRNA pools (On-TargetPlus and siGenome), and ESCC family inhibitors (MIRIDIAN Hairpin Inhibitors) were generous gifts from Dharmacon. Transfections followed the Dharmafect manufacturer's protocol. DMEM containing 1uM RNA and DMEM containing 6:1000 (v/v) Dharmafect 1 were pre-incubated at room

temperture for 5min, then mixed 1:1. After 20min of room temperature incubation, transfection mixture was added to fresh media on cells for a final RNA concentration of 100nM. For miRNA family inhibition experiments, where available, full-family LNA were used (Exiqon, miRCURY LNA, miR-181). Otherwise, cocktails of equimolar individual miRNA inhibitors were used (Dharmacon, MIRIDIAN Hairpin Inhibitors, ESCCs). The ESCC inhibitor cocktail included inhibitors of miR-302a-d, miR-291-3p, miR-294 and miR-295.

Live staining and sorting

On day 10 of reprogramming (see above), OSK-infected MEFs were treated with 5mg/mL collagenase type I (Gibco) for two consecutive 10minute incubations at 37 degrees, and then scraped. Digestion was quenched and cells washed in PBS containing 2% FBS. Cells were resuspended in PBS+2% FBS containing primary Cdh1 antibody (1:50 of 2mg/mL stock, E-cadherin monoclonal ECCD-2, Invitrogen #131900) at a maximum of 5 million cells / mL and incubated on ice for 30minutes. After washing in PBS+2%FBS, cells were treated with secondary antibody (1:200, Alexafluor 633, Invitrogen) for another 30minutes, washed again, and resuspended in 300uL PBS containing SytoxBlue (Invitrogen). Cells were sorted as live singlets into Cdh1+ and Cdh1- populations into ESC media containing 50% FBS. Of these, cells were plated at 1000 cells / well onto irradiated MEF feeder layers in standard ES +FBS media (see above). Cells were transfected the next day, then switched to ES+KSR media (see above) the next.

RT-qPCR

Total RNA was collected using either Trizol (manufacture's protocol) or RNeasy spin columns (Qiagen, manufacture's protocol). For mRNA amplification, RNA (1-5ug) was treated with DNAse I (Invitrogen) and reverse transcribed using the Superscriptase III kit (Invitrogen, manufacture's protocol) with polyT primers. Total cDNA was diluted 1:5 and 1uL per reaction was amplified using gene specific primer sets (500nM) and Power SYBR Green PCR master mix (ABI). Endogenous and exogenous Oct4, Sox2, and Klf4 primers were previously described[15]. New primer sets are listed in Supplementary Table 3. Specificity of all primer sets was verified through analysis of disassociation curves in experimental, no RT, and water only samples. For miRNAs, qRT-qPCR was performed by polyadenylating the miRNAs and using a modified polyT RT primer as previously described[34].

Immunofluorescence

Cells were fixed for 15 minutes in 4% PFA, washed in PBT (PBS + 0.1% Triton x-100), incubated for one hour at room temperature with blocking buffer (PBT+1% goat serum+2% BSA), then incubated overnight at 4 degrees in primary antibody in blocking buffer as follows: Nanog 1:50 (Abcam ab21603), SSEA1 1:100 (Univ of Iowa MC-480), Ecad 1:120 (BD Transduction Laboratories 610181), beta-Catenin 1:100 (Cell Signaling 9587). For Nanog antibody, cells were also fixed with methanol at -20 degrees C for 5 min, prior to block. Cells were then washed in PBT, incubated for one hour at room temperature in secondary antibody in blocking buffer (Alexa Fluor 1:1000 Invitrogen), washed in PBT with Hoechst 33342 1:10000 (Invitrogen), and stored in PBS before imaging.

Statistical Analysis

For small scale experiments performed in three or more independent experiments p-values were calculated using a student's t-Test.

For large-scale siRNA screens, strictly standardized mean difference (SSMD) was calculated to compare single experimental wells to either i) sets of four matched scrambled siRNA transfected wells (Fig 4a and Fig 5), ii) sets of sixteen matched mock transfection wells (Fig 1b) or iii) pair-wise sets of individual siRNA with control siRNA (Fig 6) as described previously[27].

For microarrays, total RNA from three experiments was analyzed using MouseRef-8 v2.0 Expression BeadChips through the UCLA Neuroscience Genomics Core. Data were quantile normalized using BeadArray, and statistically significant changes in gene expression between sets ($p<0.05$) were determined using Limma[35,36].

Generation of miRNA predicted target lists

Lists of genes significantly down-regulated by either miR-294 or miR-181 were obtained from previous publications. Specifically, for miR-294, microarrays were used to measure mRNA down-regulation upon addition of miR-294 to *DGCR8*−/− mESCs[32]. For miR-181, SILAC analysis was used to measure protein down-regulation upon addition of miR-181 to HeLa cells[3]. In both cases, authors' cut-offs for significant down regulation were used. To these lists, known miR-294 family or miR-181 family targets were added. Genes were then required to have miR-294 or miR-181 binding sites in mouse, and to be expressed during the course of MEF to iPSC reprogramming[43].

Luciferase Assays

All experiments were performed using the Dual-Luciferase Reporter Assay System (Promega) on a dual-injecting SpectraMax L (Molecular Devices) luminometer according to the manufacturer's protocol. Ratios of Renilla luciferase readings to firefly luciferase readings were averaged for each experiment. Replicates performed on separate days were mean centered with the readings from the individual days.

B-catenin reporter assay: Topflash reporter plasmid was obtained from Addgene (plasmid 12456)[49]. Mouse embryonic fibroblasts were cultured in Oct4, Sox2 and Klf4 reprogramming conditions described above. 24h post retroviral infection, cells were transfected with miRIDIAN miRNA mimics (Dharmacon) using Dharmafect1 (Dharmacon) as described above. 72h post retroviral infection, cells were transfected with TOPFlash reporter plasmid (final concentration 1ng/μl) and TK-renilla transfection control plasmid (Promega) (final concentration 0.33ng/μl) using Promega Fugene6 transfection reagent according to manufacturer's protocol. Recombinant murine Wnt3a (R&D biosystems) was added to the transfection mix at a final concentration of 25ng/ml in ESC media. The cells were lysed 24h after TOPFlash transfection/Wnt3a stimulation, and the luciferase assay was performed.

Target verification reporter assay: 3′UTRs of indicated genes were amplified from the mouse genomic DNA cells using the Zero Blunt TOPO (Invitrogen) vector and subcloned into psiCHECK -2 vector (Promega) using the Cold Fusion Cloning Kit (System Biosciences). 3′UTR seed sequences were mutated using the Quickchange Lightning kit (Agilent). For transfection, 8,000 miRNA-deficient Dgcr8 / mouse ESCs were plated in ESC media onto a 96-well plate pretreated with 0.2% gelatin. The subsequent day, the cells were transfected with miRIDIAN miRNA mimics (Dharmacon) using Dharmafect1 (Dharmacon) at the manufacturer's recommended concentration of 100 nM. Simultaneously, 200 ng of the psiCHECK-2 construct was transfected into the ESCs using Fugene6 (Roche) transfection reagent according to the manufacturer's protocol. Transfection of each construct was performed in triplicate in each assay. The cells were lysed 24h after transfection, and the luciferase assay was performed.

Western Blot Analysis

MEFs were cultured in Oct4 Sox2 Klf4 reprogramming conditions as described above. 24h post retroviral infection, cells were transfected with miRIDIAN miRNA mimics (Dharmacon) with Dharmafect1 (Dharmacon) as described above. 72h post infection, cells were either serum starved (high glucose (H-21) DMEM, 0.5% FBS, non-essential amino acids, L-glutamine, Penn/Strep, 55uM beta-mercaptoethanol) or media was changed to regular ESC media. For some assays, 16hrs after serum starvation / media change, serum starved cells were stimulated with IGF1 protein (Abcam) for five minutes at a concentration of 6nM in serum starvation media. Lysates were collected in lysis buffer (25 mM Tris-HCl, pH 7.9, 150 mM NaCl, 0.1% Nonidet P-40, 0.1 mM EDTA, 10% Glycerol, 1mM DTT) containing 1× protease inhibitor cocktail (Roche) and 1xPhosSTOP Phosphatase Inhibitor Cocktail (Roche). Lysates were incubated at 4°C for 10 min rocking then collected by scraping. After three snap freeze-thaw cycles, lysate was spun at 4°C and approximately 20,000*g* in a table-top centrifuge. Protein was quantified using a Bio-Rad protein assay (Bio-Rad). Five micrograms of protein was resolved on a 10% SDS PAGE gel. Proteins were transferred to Immobilon-FL (Millipore) and processed for immunodetection. Blots were scanned on a Licor Odyssey Scanner (Licor). Antibodies were diluted as follows: GAPDH 1:5,000 (Santa Cruz, sc-25778), Phospho-Akt (Ser473) 1:2000 (Cell Signaling, #4060), Phospho-Akt (Thr308) 1:1000 (Cell Signaling, #2965), Akt (pan) 1:1000 (Cell Signaling, #2920), PTEN 1:2000 (Cell Signaling, #9552), Dpysl2/Crmp2 1:1000 (Cell Signaling, #9393) Phospho-Smad2 (Ser465/467) 1:1000 (Cell Signaling, #3108), Smad2 1:1000 (Cell Signaling, #3103). Secondary infrared-dye antibodies from Licor were used at 1:25,000. Images were quantified using Odyssey Software. Original images of blots used in this study can be found in Supplementary Figure 7.

MicroRNA mimic stability assays

The miR-302 sponge consists of complementary sequences to mature miR-302b miRNA with mismatches corresponding to basepairs 9–12 of the mature miRNA. miR-302b sponge sequence corresponding to basepairs 9–11 of the mature miRNA sequence were designed to be identical and a basepair corresponding to 12 was removed from the sponge. The intentional mismatches and deleted basepair in the sponge sequence were designed to induce a bulge in the basepairing between the mature miRNA and the sponge sequence to prevent

endonucleolytic cleavage such as those occurring from exact basepairing siRNAs. The sponge sequence is CTACTAAAACACCTAGCACTTA. This sequence was repeated seven times with random 8 bp sequences between each repeated sponge site. The 7X miR-302b sponge fragment was cloned downstream of GFP in the pSIN construct using MluI and NsiI restriction sites.

NIH 3T3 fibroblasts were infected with GFP-302-sponge-puro lentivirus supernatant with 4ug/mL polybrene. After 24h, media was replaced by MEF media. After 48h, cells were split to 40% confluency and puromycin (1μg/ml) was added to this and subsequent media changes. After 10 days, foci of puromycin resistant fibroblast colonies became visible. Cells were grown to high confluency and frozen for subsequent experiments. GFP-302-sponge stably expressing fibroblasts were plated at a confluency of 300,000 cells per 6-well dish in MEF media and puromycin (1μg/ml). The subsequent day, the cells were transfected with miRIDIAN miRNA mimics (Dharmacon) with Dharmafect1 (Dharmacon) at the manufacturer's recommended concentration of 100 nM. For 10 days following transfection, GFP expression was assessed using FITC-Intensity measurement by flow cytometry (LSRII BD) and fluorescence microscopy. Cells were kept at constant confluency by 1:3 split every 24h.

Animal Use

All animal experiments described in this article were approved by the Institutional Animal Care and Use Committee of the University of California San Francisco.

Supplementary Material

Refer to Web version on PubMed Central for supplementary material.

Acknowledgments

We would like to thank C. Belair, M. Cook, R. Krishnakumar, M. La Russa, M. Shveygert and other members of the Blelloch lab for critical reading of the manuscript. We would like to thank A. Amiet (Dharmacon Thermo Scientific) for providing miRNA and siRNA libraries and M. McMahon (University of California, San Francisco, San Francisco, California, USA) for AKT expression constructs. We would like to thank H. Zhang for assistance with the high content analysis, J. Paquette, R. Bell, and A. Diaz for advice concerning our statistical methods, A. Shenoy for bioinformatic assistance, and M. Kissner for flow cytometric assistance. This work was supported by funds to R.B from the National Institutes of Health (R01:GM101180), the Leona M. and Harry B. Helmsley Charitable Trust (09PG-T1D002) and the California Institute of Regenerative Medicine (RN2-00906-1). R.L.J. is supported by the National Science Foundation (NSF) graduate research fellowship.

References

1. Fabian MR, Sonenberg N. The mechanics of miRNA-mediated gene silencing: a look under the hood of miRISC. Nature Structural Molecular Biology. 2012; 19:586–593.
2. Bartel DP. Review MicroRNAs: Target Recognition and Regulatory Functions. Cell. 2009; 136:215–233. [PubMed: 19167326]
3. Baek D, et al. The impact of microRNAs on protein output. Nature. 2008; 455:64–71. [PubMed: 18668037]
4. Selbach M, et al. Widespread changes in protein synthesis induced by microRNAs. Nature. 2008; 455:58–63. [PubMed: 18668040]
5. Guo H, Ingolia NT, Weissman JS, Bartel DP. Mammalian microRNAs predominantly act to decrease target mRNA levels. Nature. 2010; 466:835–840. [PubMed: 20703300]

6. Lim LP, et al. Microarray analysis shows that some microRNAs downregulate large numbers of target mRNAs. Nature. 2005; 433:769–773. [PubMed: 15685193]
7. Leung AK, et al. Genome-wide identification of Ago2 binding sites from mouse embryonic stem cells with and without mature microRNAs. Nature structural & molecular biology. 2011
8. Subramanyam D, Blelloch R. From microRNAs to targets: pathway discovery in cell fate transitions. Current opinion in genetics development. 2011; 21:498–503. [PubMed: 21636265]
9. Christodoulou F, et al. Ancient animal microRNAs and the evolution of tissue identity. Nature. 2010; 463:1084–1088. [PubMed: 20118916]
10. Farh KK, et al. The widespread impact of mammalian MicroRNAs on mRNA repression and evolution. Science (New York, NY). 2005; 310:1817–1821.
11. Takahashi K, Yamanaka S. Induction of pluripotent stem cells from mouse embryonic and adult fibroblast cultures by defined factors. Cell. 2006; 126:663–676. [PubMed: 16904174]
12. Samavarchi-Tehrani P, et al. Functional genomics reveals a BMP-driven mesenchymal-to-epithelial transition in the initiation of somatic cell reprogramming. Cell stem cell. 2010; 7:64–77. [PubMed: 20621051]
13. Buganim Y, et al. Single-cell expression analyses during cellular reprogramming reveal an early stochastic and a late hierarchic phase. Cell. 2012; 150:1209–22. [PubMed: 22980981]
14. Polo JM, et al. A molecular roadmap of reprogramming somatic cells into iPS cells. Cell. 2012; 151:1617–32. [PubMed: 23260147]
15. Judson RL, Babiarz JE, Venere M, Blelloch R. Embryonic stem cell-specific microRNAs promote induced pluripotency. Nature biotechnology. 2009; 27:459–461.
16. Subramanyam D, et al. Multiple targets of miR-302 and miR-372 promote reprogramming of human fibroblasts to induced pluripotent stem cells. Nature biotechnology. 2011
17. Liao B, et al. MicroRNA cluster 302-367 enhances somatic cell reprogramming by accelerating a mesenchymal-to-epithelial transition. The Journal of Biological Chemistry. 2011; 286:17359–17364. [PubMed: 21454525]
18. Anokye-Danso F, et al. Highly efficient miRNA-mediated reprogramming of mouse and human somatic cells to pluripotency. Cell stem cell. 2011; 8:376–388. [PubMed: 21474102]
19. Miyoshi N, et al. Reprogramming of mouse and human cells to pluripotency using mature microRNAs. Cell stem cell. 2011; 8:633–638. [PubMed: 21620789]
20. Banito A, et al. Senescence impairs successful reprogramming to pluripotent stem cells. Genes & development. 2009; 23:2134–2139. [PubMed: 19696146]
21. Hu S, et al. MicroRNA-302 Increases Reprogramming Efficiency via Repression of NR2F2. Stem cells Dayton Ohio. 2012
22. Li Z, Yang C, Nakashima K, Rana TM. Small RNA-mediated regulation of iPS cell generation. The EMBO Journal. 2011
23. Lin SL, et al. Regulation of somatic cell reprogramming through inducible mir-302 expression. Nucleic Acids Research. 2011; 39:1054–1065. [PubMed: 20870751]
24. Wernig M, Meissner A, Cassady JP, Jaenisch R. c-Myc is dispensable for direct reprogramming of mouse fibroblasts. Cell stem cell. 2008; 2:10–12. [PubMed: 18371415]
25. Nakagawa M, et al. Generation of induced pluripotent stem cells without Myc from mouse and human fibroblasts. Nature Biotechnology. 2008; 26:101–106.
26. Blelloch R, Venere M, Yen J, Ramalho-Santos M. Generation of induced pluripotent stem cells in the absence of drug selection. Cell stem cell. 2007; 1:245–247. [PubMed: 18371358]
27. Zhang XD, et al. The use of strictly standardized mean difference for hit selection in primary RNA interference high-throughput screening experiments. Journal of biomolecular screening the official journal of the Society for Biomolecular Screening. 2007; 12:497–509.
28. Pfaff N, et al. miRNA screening reveals a new miRNA family stimulating iPS cell generation via regulation of Meox2. EMBO Reports. 2011; 12:1154–1160.
29. Houbaviy HB, Murray MF, Sharp PA. Embryonic stem cell-specific MicroRNAs. Developmental cell. 2003; 5:351–358. [PubMed: 12919684]
30. Marson A, et al. Connecting microRNA genes to the core transcriptional regulatory circuitry of embryonic stem cells. Cell. 2008; 134:521–533. [PubMed: 18692474]

31. Chen J, et al. Synergetic Cooperation of microRNAs with Transcription Factors in iPS Cell Generation. PLoS ONE. 2012; 7:e40849. [PubMed: 22808276]
32. Melton C, Judson RL, Blelloch R. Opposing microRNA families regulate self-renewal in mouse embryonic stem cells. Nature. 2010; 463:126.
33. O'loghlen A, et al. MicroRNA Regulation of Cbx7 Mediates a Switch of Polycomb Orthologs during ESC Differentiation. Stem Cell. 2012; 10:33–46.
34. Shi R, Chiang V. Facile means for quantifying microRNA expression by real-time PCR. Biotechniques. 2005; 39:519–525. [PubMed: 16235564]
35. Dunning MJ, Smith ML, Ritchie ME, Tavare S. beadarray: R classes and methods for Illumina bead-based data. Bioinformatics. 2007; 23:2183–4. [PubMed: 17586828]
36. Smyth GK. Limma: Linear Models for Microarray Data. Bioinformatics. 2005:397–420.
37. Poliseno L, et al. Identification of the miR-106b~25 microRNA cluster as a proto-oncogenic PTEN-targeting intron that cooperates with its host gene MCM7 in transformation. Science signaling. 2010; 3:ra29. [PubMed: 20388916]
38. Cichocki F, et al. Cutting Edge: MicroRNA-181 Promotes Human NK Cell Development by Regulating Notch Signaling. The Journal of Immunology. 2011; 187:6171–6175. [PubMed: 22084432]
39. Ji J, et al. Identification of microRNA-181 by genome-wide screening as a critical player in EpCAM-positive hepatic cancer stem cells. Hepatology (Baltimore, Md). 2009; 50:472–480.
40. Wang Y, et al. Transforming growth factor-β regulates the sphere-initiating stem cell-like feature in breast cancer through miRNA-181 and ATM. Oncogene. 2010
41. Wang B, et al. TGFbeta-mediated upregulation of hepatic miR-181b promotes hepatocarcinogenesis by targeting TIMP3. Oncogene. 2010; 29:1787–1797. [PubMed: 20023698]
42. Grimson A, et al. MicroRNA targeting specificity in mammals: determinants beyond seed pairing. Molecular Cell. 2007; 27:91–105. [PubMed: 17612493]
43. Mikkelsen T, et al. Dissecting direct reprogramming through integrative genomic analysis. Nature. 2008; 454:49–55. [PubMed: 18509334]
44. Wang Y, et al. Embryonic stem cell-specific microRNAs regulate the G1-S transition and promote rapid proliferation. Nature Genetics. 2008; 40:1478–1483. [PubMed: 18978791]
45. Marson A, et al. Wnt signaling promotes reprogramming of somatic cells to pluripotency. Cell stem cell. 2008; 3:132–5. [PubMed: 18682236]
46. Maherali N, Hochedlinger K. Tgfbeta signal inhibition cooperates in the induction of iPSCs and replaces Sox2 and cMyc. Current biology: CB. 2009; 19:1718–1723. [PubMed: 19765992]
47. Ichida JK, et al. A Small-Molecule Inhibitor of Tgf-β Signaling Replaces Sox2 in Reprogramming by Inducing Nanog. Stem Cell. 2009; 5:491–503.
48. Redmer T, et al. E-cadherin is crucial for embryonic stem cell pluripotency and can replace OCT4 during somatic cell reprogramming. EMBO Reports. 2011; 12:720–726. [PubMed: 21617704]
49. Veeman MT, Slusarski DC, Kaykas A, Louie SH, Moon RT. Zebrafish Prickle, a Modulator of Noncanonical Wnt / Fz Signaling, Regulates Gastrulation Movements. Current Biology. 2003; 13:680–685. [PubMed: 12699626]
50. Kohn AD, et al. Construction and characterization of a conditionally active version of the serine/threonine kinase Akt. The Journal of biological chemistry. 1998; 273:11937–11943. [PubMed: 9565622]
51. Yu Y, et al. Stimulation of Somatic Cell Reprogramming by Eras-Akt-Foxo1 Signaling Axis. Stem cells Dayton Ohio. 2013
52. Liao J, et al. Inhibition of PTEN Tumor Suppressor Promotes the Generation of Induced Pluripotent Stem Cells. Molecular therapy: the journal of the American Society of Gene Therapy. 2013
53. Menendez S, Camus S, Belmonte JCI. p53: Guardian of reprogramming. Cell Cycle. 2010; 9:3887–3891. [PubMed: 20948296]
54. Vazquez-martin A, et al. Activation of AMP-activated protein kinase (AMPK) provides a metabolic barrier to reprogramming somatic cells into stem cells c 2012 Landes Bioscience. c 2012 Landes Bioscience. Cell cycle Georgetown Tex. 2012; 11:974–989.

55. Jin L, et al. Ubiquitin-dependent regulation of COPII coat size and function. Nature. 2012; 482:495–500. [PubMed: 22358839]

56. Jayawardena TM, et al. MicroRNA-mediated in vitro and in vivo direct reprogramming of cardiac fibroblasts to cardiomyocytes. Circulation research. 2012; 110:1465–73. [PubMed: 22539765]

57. Yoo AS, et al. MicroRNA-mediated conversion of human fibroblasts to neurons. Nature. 2011

58. Nam, Y., et al. Reprogramming of human fibroblasts toward a cardiac fate. 2013. / DCSupplemental.www.pnas.org/cgi/doi/10.1073/pnas.1301019110

59. Park CY, Choi YS, McManus MT. Analysis of microRNA knockouts in mice. Human Molecular Genetics. 2010; 19:R169–R175. [PubMed: 20805106]

60. Ebert MS, Sharp PA. Roles for MicroRNAs in Conferring Robustness to Biological Processes. Cell. 2012; 149:515–524. [PubMed: 22541426]

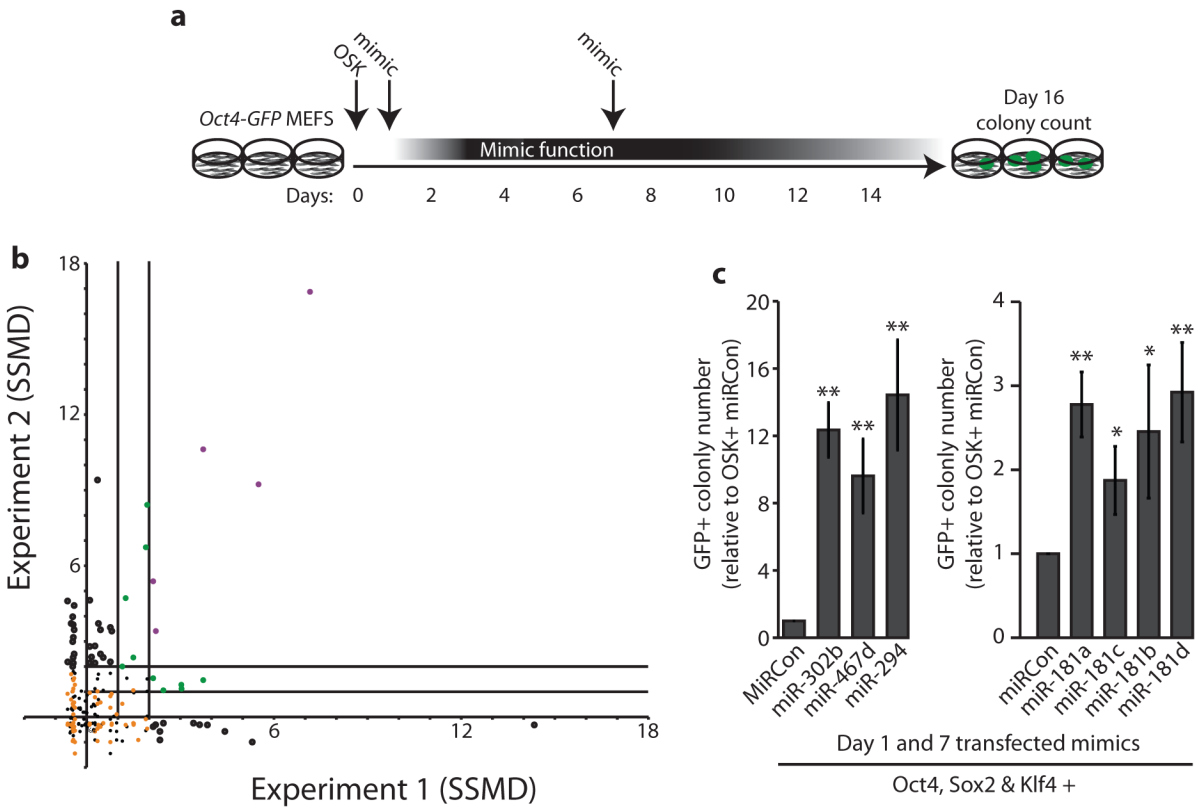

Figure 1. A genome-wide screen identifies verified and novel miRNA enhancers of OSK reprogramming

a) Schematic representation of screen for miRNA enhancers of OSK-reprogramming, and mimic duration (details in Supp. Fig. 1). b) Results of biological duplicate genome-wide screens for miRNA mimics that enhance OSK-reprogramming. Data points represent SSMD between the number of Oct4-GFP+ colonies on day 16 in the presence of an exogenous miRNA mimic compared to 16 mock transfections per plate (shown as orange dots). Significance defined as strong (SSMD>2), moderate (SSMD>1), or weak (SSMD <1). Large dots represent SSMD >2 in at least one experiment with purple being strong in both and green being strong in one and moderate in second experiment (miRNAs corresponding to purple and green dots are shown in inlay). All significant results listed in Supplentary Table 1a. c) Verification of two miRNA families. MiRNA mimics transfected at days 1 and 7. Data represents number of day 16 Oct4-GFP+ colonies from OSK-reprogramming supplemented with indicated miRNA, relative to OSK + non-targeting miRNA mimic (MirCon). Error bars, s.e.m. (n = 3 biological replicates). Replicates performed with separate preparations of virus and MEFs. *=p<0.05, **=p<0.005 by two-tailed Student's t-test.

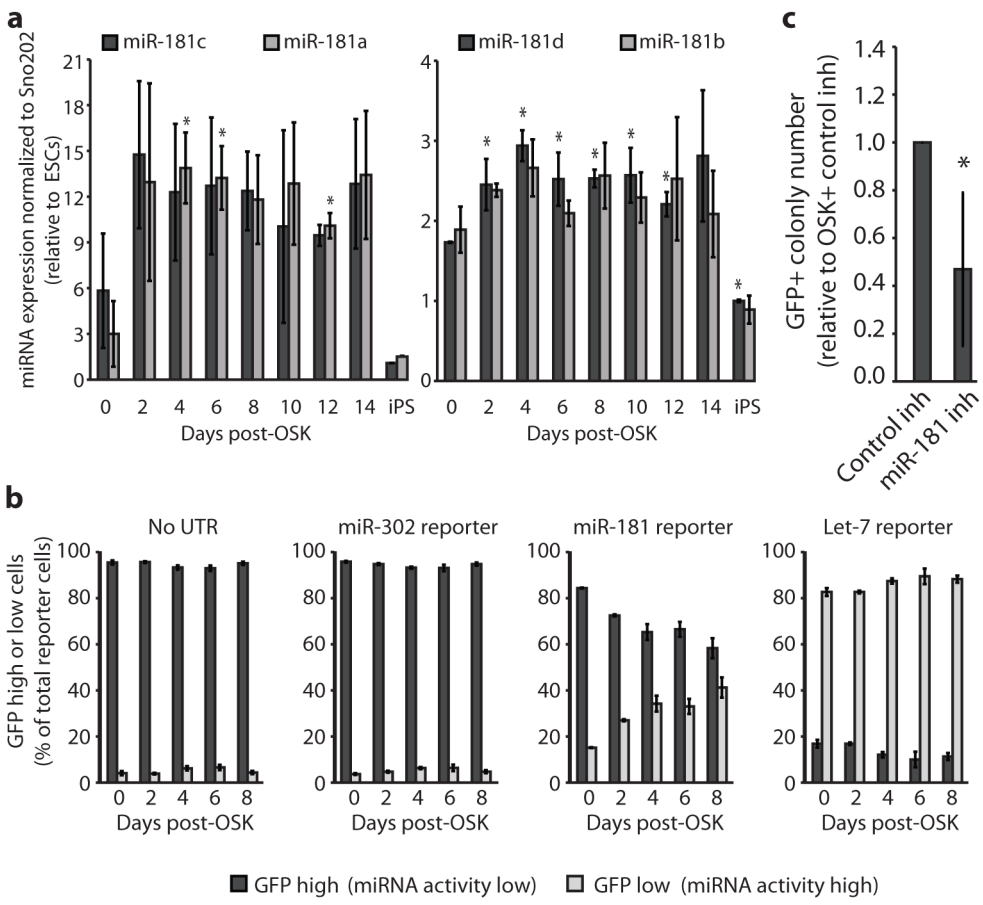

Figure 2. The miR-181 family is an OSK-activated positive regulator of reprogramming

a) RT-qPCR analysis for individual members of miR-181 family during reprogramming. (n = 3 biological replicates). b) Quantification of flow cytometric analysis measuring GFP expression from miRNA reporters as in Supp. Fig. 1. Endogenous miRNA during OSK-reprogramming was measured. High GFP expression indicates low miRNA expression and vice versa. (n = 3 biological replicates). c) OSK-reprogramming as in Fig. 1d, but with miRNA family inhibitors introduced on days 1 and 5. (n = 3 biological replicates). For all experiments replicates Error bars, s.e.m. Replicates performed with separate preparations of virus and MEFs. *=$p<0.05$ by two-tailed Student's t-test.

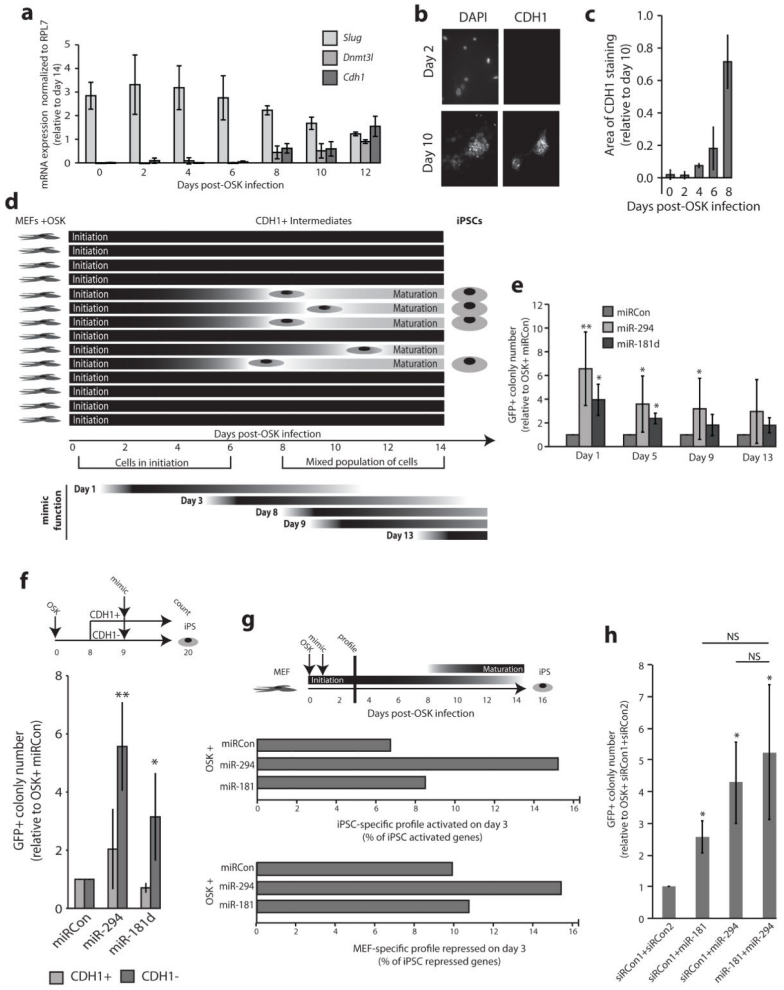

Figure 3. miR-294 and miR-181 enhance reprogramming during the early initiation phase

a) RT-qPCR analysis for markers of completed initiation in OSK-infected MEFs. (n = 4 biological replicates). B) Representative Cdh1-negative or Cdh1-positive immuno-fluorescent cells in OSK-infected MEFs on indicated days. c) Area of Cdh1-positive staining per well. (n = 4 biological replicates). d) Representation of reprogramming phases, heterogeneity of reprogramming populations, and duration of mimic function when transfected at different time points. e) Mimics were transfected at either day 1, 5, 9 or 13 post-OSK infection of MEFs. Day 20 Oct4-GFP+ colonies relative to miRCon shown for each day. (n = 4 biological replicates). g) MEFs were sorted into Ecad+ and Ecad- populations on day 8 post OSK-infection and transfected with mimic 24 hours later. Day 20 Oct4-GFP+ colonies relative to OSK+miRCon shown. (n = 3 biological replicates). h) Representation of array data comparing MEFs, MEFs infected with OSK +/− indicated mimic transfection, and iPSCs. MEF RNA collected three days after OSK-infection and 48 hours after mimic transfection. Changes in expression with an adjusted $p<0.05$ represented. (n = 3 biological replicates). Percentage of all genes activated (top) or repressed (bottom) in iPSCs as compared to MEFs shown. i) OSK-reprogramming with two miRNAs or controls (SiRCon1 or SiRCon2) transfected on day 1. Day 16 Oct4-GFP+ colonies relative to

SiRCon1+SiRCon2. (n = 7 biological replicates). For all experiments replicates Error bars, s.e.m. Replicates performed with separate preparations of virus and MEFs. *=p<0.05, **=p<0.005 by two-tailed Student's t-test.

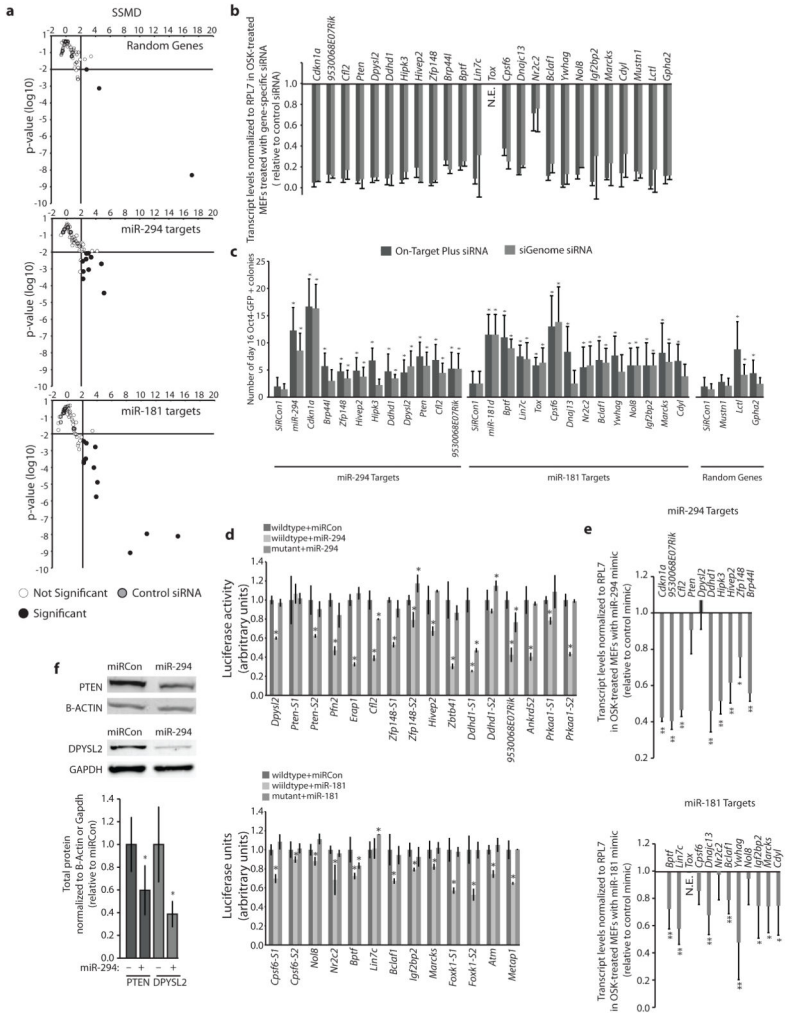

Figure 4. An unbiased screen reveals novel direct targets of miR-294 and miR-181 that inhibit reprogramming initiation

a) Effect of day 1 transfected siRNAs against miRNA targets on reprogramming efficiency. SSMD and p-values compare wells transfected with siRNA to 4 different control siRNA (grey dots) (n = 3 biological replicates). Black dots indicate significant hits (SSMD>2, p-value<0.01). b) RT-qPCR analysis of MEFs on day 3 post-OSK infection and day 2 post-transfection of OnTargetPlus (dark) or siGenome (light) siRNA pools. N.E. = no detectable expression with or without siRNA. (n = 3 biological replicates). c) Verification of hits using independent pools of siRNA transfected on day 1 of OSK-reprogramming. Number of day 16 Oct4-GFP+ colonies relative to non-targeting siRNA control (siRCon1). (n = 4 biological replicates). d) Luciferase reporter assays verifying miRNA-mediated translational repression of functional targets. Luciferase activity in cells transfected with reporters expressing either wildtype or mutant UTRs, (Supplementary Figure 4) +/− co-transfection of indicated miRNAs normalized to transfection with control miRNA (miRCon). (n = 4 technical replicates). e) RT-qPCR analysis 48 hours post-transfection with either miR-294 or miR-181 in reprogramming MEFs. (n = 3 biological replicates). f) Representative images (top) and quantification (bottom) of Westerns detecting PTEN and DPYSl2 protein +/− miR-294

during OSK-mediated reprogramming of MEFs compared to miRCon. (n = 4 biological replicates). For all experiments, biological replicates contained separate preparations of virus and MEFs. Technical replicates were independent wells and transfections. Error bars, s.e.m. *=$p<0.05$, **=$p<0.005$ by two-tailed Student's t-test.

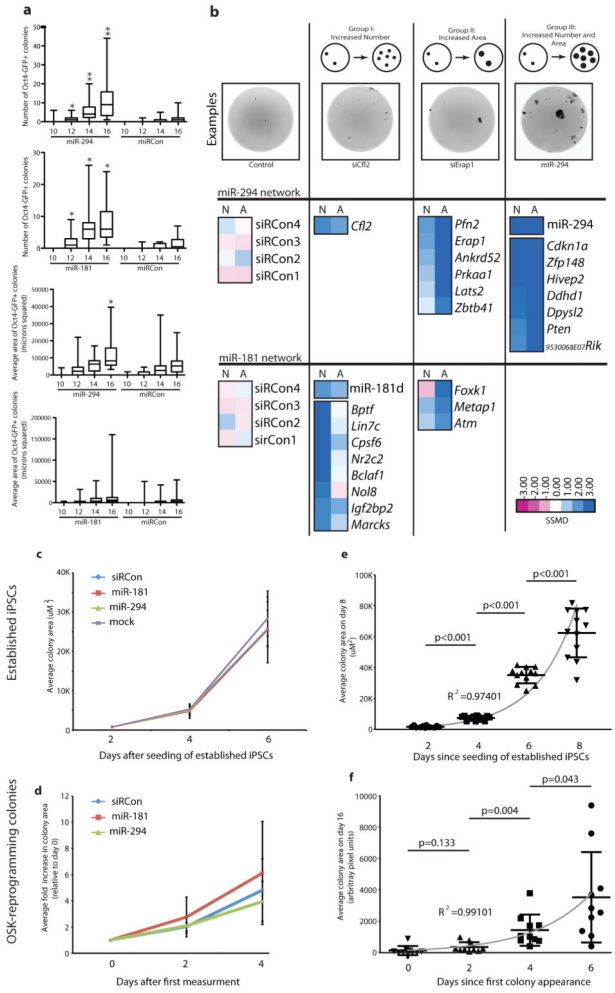

Figure 5. miR-294 and miR-181 alter both distinct and common properties of reprogramming

a) Colony number (top) and colony area (bottom) on days 10, 12, 14 and 16 post-OSK infection +/− miR-294, miR-181 or control (miRCon). Plots indicate 2.5, 50, and 97.5 percent tiles and range. (n = 3 biological replicates) b) Schematics (top row), examples (second row) and categorization (bottom two rows) of miRNAs and siRNAs based upon effects on colony formation. Heatmaps depict SSMD comparing experimental wells to controls (siRCon1-4). (n = 3 biological replicates). c) Average area of iPSC colonies followed over time, seeded as single cells and transfected with miRNAs on day 2. Averages of all colonies (~500 per experiment) of three independent iPSC lines each measured in technical quadruplicate. d) Average area of Oct4-GFP+ colonies during OSK-reprogramming transfected with miRNAs. Wells imaged every 2 days and area measured for 96 hours after the first day colony was visible. Averages of ten individual colonies across five biological replicate experiments. e) Scatter plot of colony area in relation to days after single cell colony seeding as in c). f) Scatter plot depicting of average Oct4-GFP+ colony area during OSK-reprogramming in relation to number of days post-infection colony first detectable as in d). For all experiments, biological replicates contained separate preparations

of virus and MEFs. Technical replicates were independent wells and transfections. Error bars, s.e.m. *=p<0.05, **=p<0.005 by two-tailed Student's t-test.

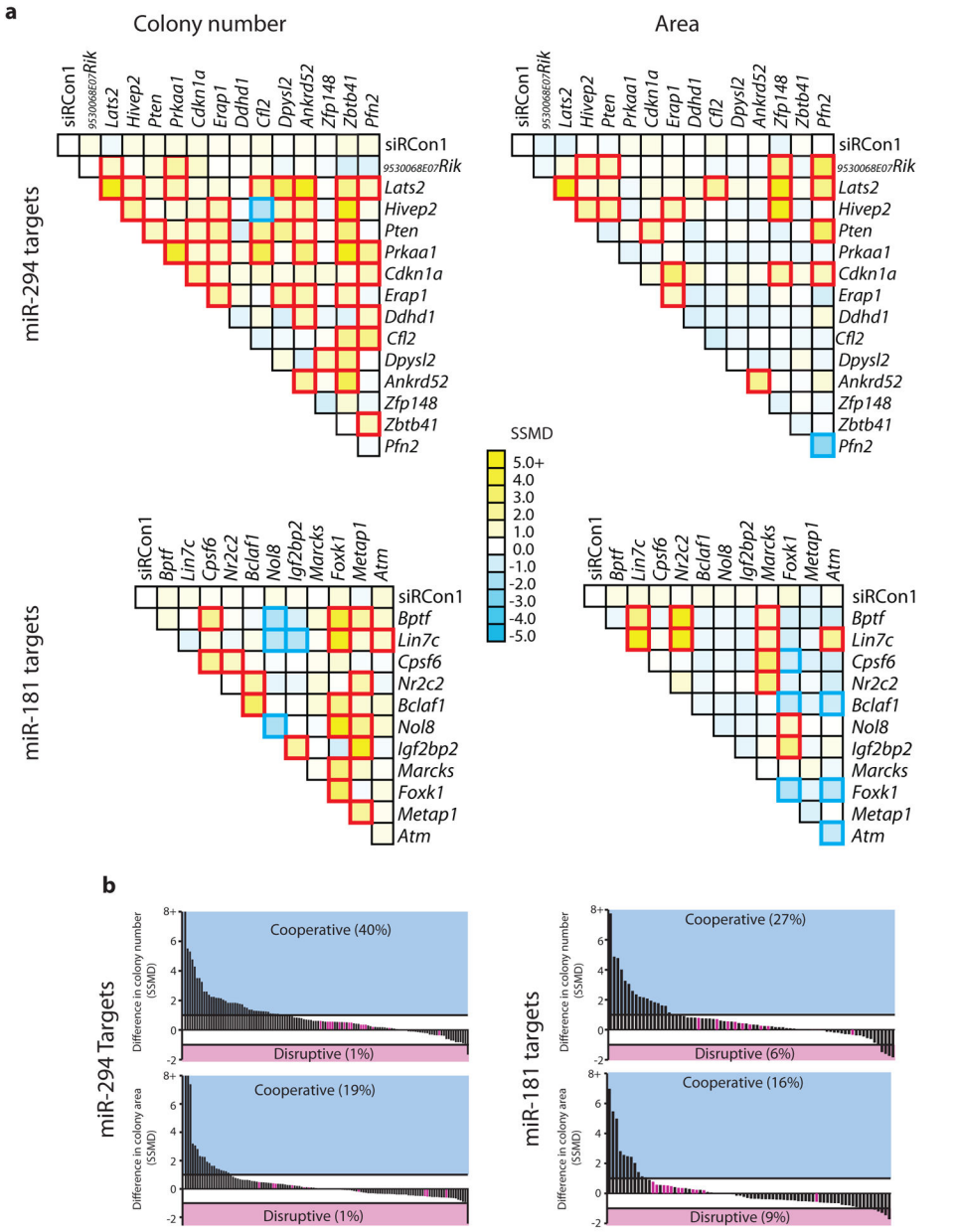

Figure 6. miRNA-targeted genes cooperate to reduce both frequency and rate of reprogramming

a) Heatmaps depicting screens for functional cooperation between siRNAs. For any combination of two siRNA, day 16 Oct4-GFP colony number or area in wells containing both siRNA, were compared to the set of wells containing only the single siRNAs or each individual siRNA in combination with control siRNA (siRCon) using SSMD. SSMD is indicated by color of box at intersection of two siRNA listed on axis. Left depicts changes in colony number. Right indicates changes in colony area. SSMD>1 (cooperative relationship) are highlighted in red borders. SSMD<-1 (disruptive relationship) are highlighted in blue borders. Screens performed in technical duplicate with independent wells and transfections. b) Quantification of relationships in a). Bars indicate every potential relationship between

siRNAs against two miR-294 (left) or miR-181 (right) targets (black bars) or between single siRNAs against targets and control siRNAs (purple bars).

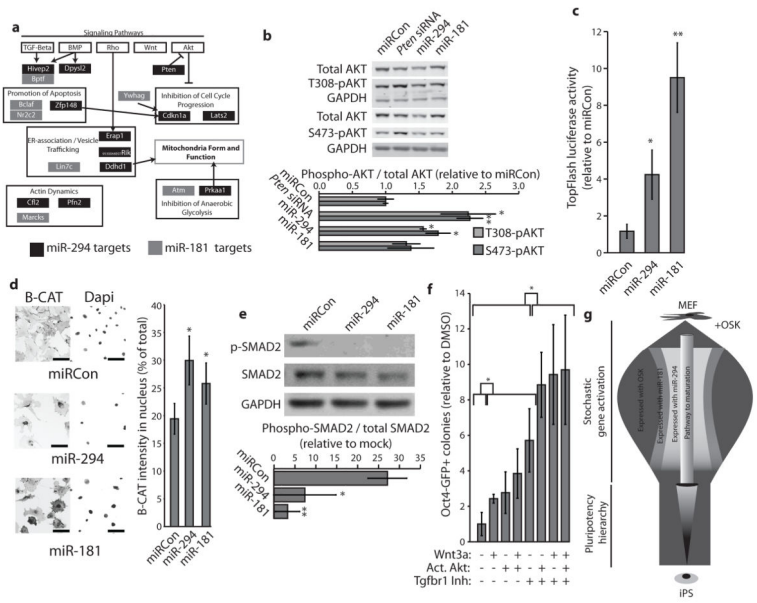

Figure 7. MiR-294 and miR-181 targets converge on cooperating pathways and processes to enhance reprogramming

a) Schematic of signaling pathways and cellular processes enriched in miR-294 and miR-181 targets. Pathways identified by predicted target enrichment are boarded in black. Functional targets shown to inhibit reprogramming known to be involved in these categories are shown in grey and black. b) Representative Western blot (top) detecting total and phoshpo-Akt levels in reprogramming MEFs +/− indicated siRNA and miRNA, serum starved for 24 hours, and treated with IGF. Quantification (bottom) (n = 3 biological replicates). c) Relative luciferase units from TopFlash reporter co-transfected into serum starved and Wnt3a-treated reprogramming MEFS with indicated miRNAs. (n = 3 biological replicates). d) Representative images (left) and quantification (right) of immuno-fluorescent B-cat staining in reprogramming MEFs treated with indicated miRNA as in c). (n = 3 biological replicates). e) Representative images (top) and quantification (bottom) of Westerns detecting SMAD2 and phospho-SMAD2 in reprogramming MEFs treated with miRNA after 24 hours serum starvation. (n = 4 biological replicates). f) Day 16 colony count of MEFs infected with OSK and treated with indicated combinations of recombinant Wnt3a, Tgfbr1 Inh and M+Akt:ER+Tamoxifen (Act. Akt) on days 2–8. (n = 4 biological replicates). g) Schematic representation of the role of miR-181 and miR-294 as inhibiting stochastic gene expression during initiation and funneling the transcriptome toward successful reprogramming. For all experiments, biological replicates contained separate preparations of virus and MEFs. Error bars, s.e.m. *=p<0.05, **=p<0.005 by two-tailed Student's t-test.